PAPER

Check for updates

Colorimetric detection of hydrogen peroxide and glucose by exploiting the peroxidase-like activity of papain†

Yuye Chen,[a] Qingmei Zhong,[a] Yilin Wang, [ID] *[ab] Chunling Yuan,[a] Xiu Qin[a] and Yuanjin Xu[a]

Papain, a natural plant protease that exists in the latex of *Carica papaya*, catalyzes the hydrolysis of peptide, ester and amide bonds. In this work, we found that papain displayed peroxidase-like activity and catalyzed the oxidation of 3,3′,5,5′-tetramethylbenzidine (TMB) in the presence of H_2O_2. This results in the formation of a blue colored product with an absorption maximum at 652 nm. The effects of experimental parameters including pH and reaction temperature on catalytic activity of papain were investigated. The increase of absorbance induced by the catalytic effect of papain offers accurate detection of H_2O_2 in the range of 5.00−90.0 μM, along with a detection limit of 2.10 μM. A facile colorimetric method for glucose detection was also proposed by combining the glucose oxidase (GOx)-catalyzed glucose oxidation and papain-catalyzed TMB oxidation, which exhibited a linear response in the range of 0.05−0.50 mM with a detection limit of 0.025 mM. The method proposed here displayed excellent selectivity, indicating that common coexisting substances (urea, uric acid, ascorbic acid, maltose, lactose and fructose) in urine did not interfere with detection of glucose. More importantly, the suggested method was successfully used to precisely detect the glucose concentration in human urine samples with recoveries over 96.0%.

1. Introduction

In clinical diagnosis, several disease-related biomolecules (such as glucose,[1] uric acid,[2] and sarcosine[3]) are generally measured *via* indirect colorimetric analysis. Namely, these biomolecules are oxidized with the catalysis of corresponding oxidase enzymes, then, hydrogen peroxide (H_2O_2) is quantitatively produced, which can yield hydroxyl radicals (·OH) by the catalysis of peroxidase (such as horseradish peroxidase, HRP). After that, the hydroxyl radical is able to oxidize 3,3′,5,5′-tetramethylbenzidine (TMB) into oxidized TMB with an absorption peak at 652 nm. Thus the content of the biomolecule can be finally determined by measuring the absorbance at 652 nm. This method does not need any sophisticated instrumentation and can achieve rapid visual detection of target molecules,[4–6] which makes it feasible, fast and cost-effective.[7,8] In addition, HRP, as a biological catalyst, possesses remarkable advantages such as high substrate specificities and high efficiency under mild conditions, which makes the method highly selective with less interference.[9] Of course, as a natural enzyme, HRP has

inherent disadvantages of high cost, difficult preparation, low stability, and easily denaturing in extreme conditions, which impedes its widespread applications.[10] Therefore, much effort has been done in exploration of peroxidase-like to replace HRP in the construction of enzymatic assays. A series of nanomaterials, including noble metals (Au,[11] Ag,[12] Pt,[13] Pd[14] and Rh[15]), transition metal oxides or chalcogenides (Fe_3O_4,[16] Co_3O_4,[17] CeO_2,[18] VS_2,[19] CuS,[20] Fe_3S_4,[21] *et al.*), and carbon-based nanomaterials,[22–25] have been reported to exhibit the highly peroxidase-like activity, which have been used as peroxidase mimetic for the detection of H_2O_2, glucose, uric acid, *etc.* Although these nano-enzymes are important, they suffer from drawbacks such as high cost, time-consuming and tedious preparation of nanomaterials. Moreover, poor stability and biocompatibility of the nanomaterials also limit their practical applications.[26] Therefore, it is quite necessary for researchers to explore new natural enzymes with wide sources and low cost, and apply them in colorimetric analysis. Zheng's group reported that ficin exhibited significant peroxidase-like activity, which had been used for colorimetric detection of glucose[27] and uric acid,[28] individually.

Papain, a natural plant protease exists in the latex of *Carica papaya*, catalyzes the hydrolysis of peptide, ester and amide bonds. It is recognized as a sulfhydryl protease, the active site is located at the interface of L- and R-domains in the form of a V shaped cleft and is formed by a cysteine, a histidine, from an asparagine and a glutamine residue.[29] Because of its good

[a]School of Chemistry and Chemical Engineering, Guangxi University, Guangxi Key Laboratory of Biorefinery, Nanning 530004, China

[b]Guangxi Key Laboratory for Agro-Environment and Agro-Product Safety, Nanning 530004, China. E-mail: theanalyst@163.com; Tel: +86 771 3392879

† Electronic supplementary information (ESI) available. See DOI: 10.1039/c9ra03111a

stability, high protein hydrolysis ability and good degradation effect on many kinds of proteins, papain, one of the industrial proteases, has been widely used in food, medicine, feed, cosmetics, leather, and textile industries.[30,31] In this work, we reported for the first time that papain exhibited significant peroxidase-like activity, which could catalyze oxidation of TMB in the presence of H_2O_2 to produce blue color. It is well known that H_2O_2 is the product of the oxidation of glucose. Therefore, a simple colorimetric method was developed for the detection of glucose based on the glucose oxidase (GOx)-catalyzed glucose oxidation and papain-catalyzed TMB oxidation (Scheme 1). And this method was applied for the detection of glucose in urine samples with satisfactory results.

2. Experimental section

2.1 Chemicals and instruments

All the chemicals in this study were of analytical grade and used as received. Papain, glucose, glucose oxidase (GOx) and 3,3′,5,5′-tetramethylbenzidine (TMB) were obtained from Macklin Biochemical Reagent (Shanghai, Co., Ltd., China). N,N-Dimethylformamide (DMF), acetic acid (HAc), sodium acetate (NaAc), hydrogen peroxide (H_2O_2), urea, uric acid, ascorbic acid, maltose, lactose, and fructose were acquired from Da Mao Chemical Reagents (Tianjin, China). TMB was dissolved in DMF, doubly deionized water (DDW) was used throughout.

Absorption spectra were recorded using a UV-4802 spectrophotometer (Unico, Shanghai, China) equipped with a 1.0 cm cuvette. The pH of the solutions was monitored with a PXSJ-216 pH meter (Shanghai Precision Science Instrument Co., Ltd., China).

2.2 Procedure for determination of H_2O_2 and glucose

H_2O_2 detection was performed as follows: 100 μL 100 μg mL^{-1} papain, 1.0 mL 5.0 mM TMB, and 1.0 mL H_2O_2 solution with different concentrations were added sequentially in 7.9 mL NaAc–HAc (pH 3.5) buffer. The mixture was incubated at 40 °C for 20 min then kept in an ice-water bath for 10 min to stop the reaction. Finally, the UV-vis spectroscopy of the resultant solution was scanned from 500 to 800 nm at room temperature, and the absorbance at 652 nm was used for quantitative analysis.

Glucose detection was carried out as follows: 0.2 mL GOx of 1.0 mg mL^{-1} and 1.0 mL of different concentrations of glucose were added into 1.0 mL phosphate buffer (pH 7.0) and then incubated at 37 °C for 40 min. Subsequently, the glucose reaction solution was added into 7.8 mL HAc–NaAc (pH 3.5) buffer

containing 0.5 mM TMB and 1.0 μg mL^{-1} papain. The mixture was incubated at 40 °C for 20 min then kept in an ice-water bath for 10 min to stop the reaction. The resultant solution was monitored by the UV-vis spectroscopy.

The selectivity of the proposed detection system was assessed by adding potential interfering substances coexisting in human urine (such as urea, uric acid, ascorbic acid, maltose, lactose, fructose) instead of glucose in a same way. The final concentrations of the interfering substances were all 8.0 μM.

2.3 Analysis of real samples

The morning urine samples were centrifuged at 12 000 rpm for 40 minutes to collect the supernatant for experiment. And then various amounts of glucose were spiked to the urine samples. Finally, the sample detection was carried out using above procedure.

3. Results and discussion

3.1 Intrinsic peroxidase-like activity of papain

The peroxidase-like activity of papain was investigated through catalytic oxidation of TMB by papain in the presence of H_2O_2 and monitoring the absorption spectra. As shown in Fig. 1, the interaction of TMB with papain in the presence of H_2O_2 leads to the formation of deep blue colored product with a strong absorption peak at 652 nm, which is similar to the typical HRP-catalyzed oxidation of TMB.[32] In contrast, the control experiment of TMB with papain in the absence of H_2O_2 does not lead to the generation of blue color (Fig. 1 inset), and TMB with H_2O_2 in the absence of papain only results in a negligible blue color, which absorbance of corresponding absorption spectra is very low at 652 nm, indicating that both papain and H_2O_2 are required for the reaction to occur. These results demonstrate that papain exhibits peroxidase-like activity, which can accelerate TMB oxidation in the presence of H_2O_2. It was reported

Scheme 1 Schematic illustration of the peroxidase-like activity of papain for the colorimetric detection of glucose by coupling with glucose oxidase (GOx) catalysis.
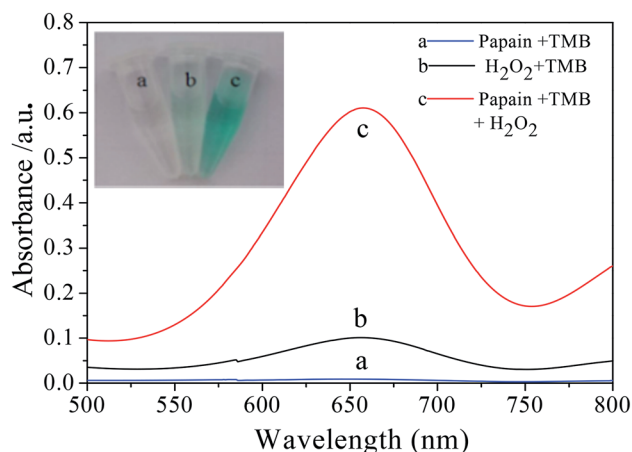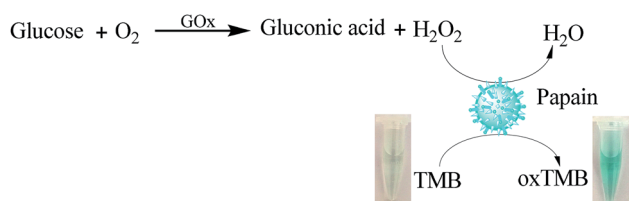
Fig. 1 Papain shows intrinsic peroxidase-like activity. The absorption spectra and colors of TMB in different reaction systems: (a) papain + TMB, (b) H_2O_2 + TMB, (c) papain + TMB + H_2O_2 (other conditions: 100 μL of 100 μg mL^{-1} papain; 1 mL of 5.0 mM TMB; 1 mL of 50 μM H_2O_2; pH = 3.5; reaction temperature is 35 °C; reaction time is 20 min.).
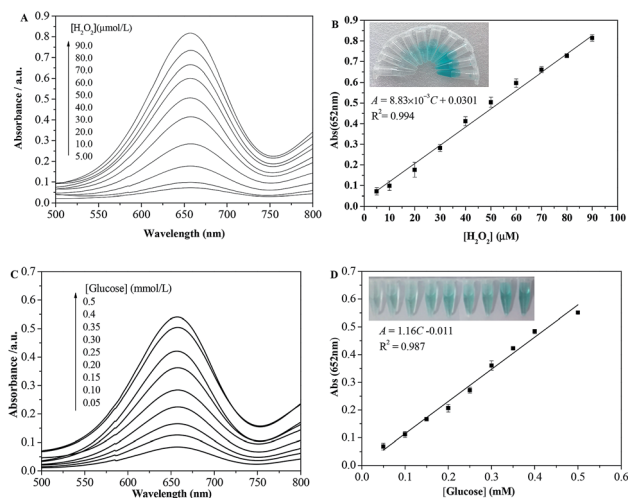
Fig. 2 (A) UV-vis absorption spectra of papain-TMB solution containing H_2O_2 concentrations varied from 5.00 to 90.0 μM. (B) The relation between the absorbance at 652 nm and the H_2O_2 concentrations. (C) UV-vis absorption spectra of glucose-GOx–TMB-papain system in the presence of different concentration of glucose. (D) The calibration curve for glucose determination. Inset: Photographs for colorimetric detection of (B) H_2O_2 and (D) glucose, respectively.

that nanomaterials with peroxidase-like activity also had the same effect.[33–35]

3.2 Steady-state kinetic analysis of papain

To further investigate the catalytic activity of the papain, apparent steady-state kinetic parameters for papain catalyzed reaction were determined by varying the concentration of TMB and H_2O_2. The experiments were performed at 40 °C using 1.0 μg mL^{-1} of papain in 0.1 M HAc–NaAc buffer (pH 3.5) containing either 5.0 mM H_2O_2 with different concentrations of TMB (0.5–3.0 mM) or 1.0 mM TMB with different concentrations of H_2O_2 (0.25–2.0 mM). After incubating for 20 minutes, the reaction was stopped with cold water. Then the absorbance of oxidized TMB at 652 nm were recorded, and the concentration of oxidized TMB were estimated using Beer–Lambert law (molar extinction coefficient, $\varepsilon = 3.9 \times 10^4$ M^{-1} cm^{-1}).[36] The reaction velocities were calculated and plotted against concentration of TMB or H_2O_2. As shown, typical Michaelis–Menten curves are observed for both TMB and H_2O_2 (Fig. S1A and B†). Double-reciprocal curves were plotted (Fig. S1C and D†) and

fitted to the equation $1/V = (K_m/V_{max}) \times (1/[S]) + (1/V_{max})$, where V is the initial velocity, V_m represents the maximal reaction velocity, [S] corresponds to the concentration of substrate and K_m is the Michaelis constant. We obtained K_m and V_{max} from the slope and intercept of the curves. The results given in Table S1† show that the K_m value of papain towards TMB and H_2O_2 both are larger than those of HRP and ficin,[37] implying that higher TMB and H_2O_2 concentrations are needed for papain to achieve maximal reaction velocity than those for HRP and ficin. The derived catalytic constant (K_{cat}) was also taken to compare the enzymatic catalytic activity. The K_{cat} values of papain with TMB and H_2O_2 as the substrates are close to those of ficin, suggesting that papain can also act as an efficient peroxidase mimic.

3.3 Optimization of experimental conditions

Similar to the nature of enzymes and other nanomaterials based mimics, the catalytic activity of papain is dependent on pH, temperature, and time. In this work, the peroxidase-like activity of papain was evaluated at different pH (from 2.5 to 5.5), incubation temperature (25 to 50 °C), and incubation time (from 5 to 30 min).

Papain is a kind of biological catalyst, easily denatured at unsuitable pH values or high temperature. Therefore, the catalytic activity of papain is remarkably influenced by pH and incubation temperature. As shown in Fig. S2,† an increase in pH from 2.5 to 3.5 results in the increased absorbance whereas a further increase in pH from 3.5 to 4.5 leads to a gradual decrease. The maximum of absorbance is obtained at pH 3.5, indicating that the oxidation of TMB occurs under weakly acidic condition, which is consistent with that reported for the oxidation of TMB and thus the pH is adopted. The incubation temperature-dependent response curve is shown in Fig. S3.† The catalytic activity of papain greatly increases as the incubation temperature increases from 25 to 40 °C. Further increase in temperature gives rise to a decrease in catalytic activity, attributed to the inactivation of papain at high temperature. The effect of incubation time was optimized (Fig. S4†). A longer incubation time enables the substrate TMB to react with H_2O_2 more completely. The increase of absorbance slows down obviously when the incubation time exceeds 20 min. Therefore, the optimal pH value, incubation temperature, and incubation time are 3.5, 40 °C, and 20 min, respectively.

Table 1 Comparison of different methods for glucose detection

Method	Materials	Linear range (μM)	Detection limit (μM)	Ref.
Fluorimetry	SGOx-NFs-Amplex Ultra Red	0–100	3.5	38
Fluorimetry	MnO_2-PFR NPs	5–1000	1.5	39
Fluorimetry	WS_2 QDs	1–60	0.3	40
Fluorimetry	Mn-doped $Zn_{0.5}Cd_{0.5}S@ZnS$ NRs	50–300	0.1	41
Colorimetry	$Cu_2(OH)_3Cl$–CeO_2 NPs-TMB	100–2000	50	42
Colorimetry	Fe_3O_4/graphene NPs-TMB	5–500	0.8	43
Colorimetry	GQDs/CuO NPs-TMB	2–100	0.59	44
Colorimetry	N-GQDs-TMB	25–375	16	45
Colorimetry	Papain-TMB	50–500	25	This work

3.4 Detection of H$_2$O$_2$ and glucose

Since the absorbance of oxidized TMB at 652 nm was associated with H$_2$O$_2$ concentration, a simple method was developed for the detection of H$_2$O$_2$ spectrophotometrically. Fig. 2A displays the UV-vis absorption spectra of papain-TMB solution containing H$_2$O$_2$ with different concentrations. As seen, the absorbance at 652 nm increases with the increase of H$_2$O$_2$ concentration, and fits a linear regression equation of $A = 8.83 \times 10^{-3}C + 0.0301$ over the range of 5.00–90.0 μM (Fig. 2B). The limit of detection for H$_2$O$_2$ is calculated to be 2.10 μM ($3\sigma/k$), showing a high sensitivity for H$_2$O$_2$ analysis. Simultaneously, the color change of the solution is obvious and easily observed by the naked-eye (Fig. 2B inset). As H$_2$O$_2$ is the main product of GOx-catalyzed glucose oxidation, colorimetric detection of glucose can be realized when the papain-catalyzed TMB oxidation is coupled with the GOx-catalyzed glucose oxidation. Fig. 2C presents the UV-vis absorption spectra for glucose detection under the optimal conditions and the absorbance at 652 nm increases gradually with the increase of glucose concentration. As observed in Fig. 2D, the absorbance is proportional to the glucose concentration ranging from 0.05 to 0.50 mM with the detection limit of 0.025 mM glucose. The linear regression equation is $A = 1.16C$ (mM) $- 0.011$ with a correlation coefficient of 0.987. Moreover, the color variation for the glucose response is also obvious by visual observation (Fig. 2D inset).

In Table 1, we compared the analytical performance of the proposed method with those reported methods. As described in Table 1, the linear range of our method is wider than or comparable to some of theirs. Although the detection limit of our method is not the lowest, it provides an alternative method for the detection of glucose in real samples. It is remarkable that almost all of the reported methods require the preparation of probes or nanomaterials while our method does not need.
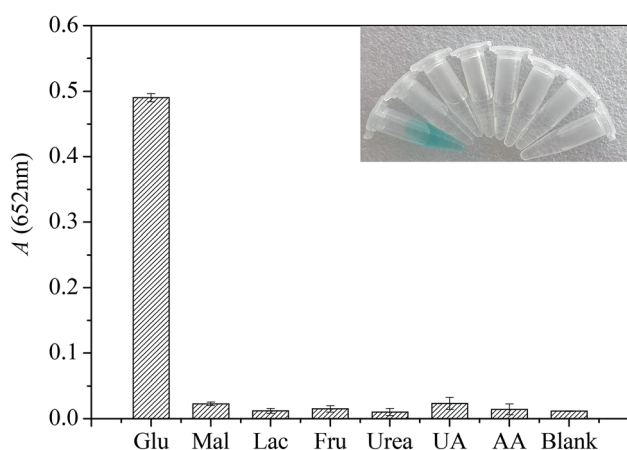

Fig. 3 Selectivity of the proposed method for the detection of glucose. Each potential interfering substance was separately added into reaction solution in the absence of glucose. The concentration of glucose was 0.4 mM, and the concentration of the potential interfering substances was 8.0 mM. Inset: Typical photograph of glucose detection with the colorimetric method using GOx and papain as the catalysts (from left to right: glucose, maltose, lactose, fructose, urea, uric acid, ascorbic acid and blank).

Table 2 Determination results of glucose in urine samples ($n = 3$)

Sample	Addition/(mM)	Recovery/(mM)	RSD/%	Recovery/%
1	0.10	0.097	3.2	96
2	0.20	0.21	2.4	104
3	0.30	0.31	2.6	104

Thus it can be derived the suggested method is fast and convenient.

In order to evaluate the selectivity of glucose detection, control experiments were conducted with potential interfering substances with urea, uric acid (UA), ascorbic acid (AA), maltose (Mal), lactose (Lac) and fructose (Fru) in solution at concentration of 8.0 mM. As shown in Fig. 3, only the addition of glucose can induce a dramatic change in absorbance and an obvious color change (Fig. 3 inset), whereas little changes are observed in the presence of other interference substances, even the concentration of these substances is 20-fold higher than that of glucose. The results clearly indicate that those existing interferences are inert to glucose detection, hinting that the present method displays a high selectivity toward glucose. Therefore, this study proposed colorimetric analysis method does not require complicated sample processing and can be used for selective detection of glucose in urine samples.

3.5 Analytical applications

Based on the activity of papain's peroxidase and glucose oxidase, this method has been successfully used in the detection of glucose in human urine samples from healthy volunteers who are three of our research group. Before the test, morning urine was taken and the supernatant was centrifuged for 40 minutes at a speed of 12 000 rpm for analysis. The results of the determination and recovery are shown in Table 2. It is found that the average recoveries of the glucose are in the range of 96% to 104%, and the relative standard deviation values of the measurements are from 2.4% to 3.2%. High recovery and good precision of glucose determination suggest that the proposed colorimetric method can greatly reduce the matrix effect of the human urine sample. These results clearly indicate the feasibility of this method for the determination of glucose in biological samples.

4. Conclusions

In conclusion, we reported for the first time that papain exhibited significant peroxidase-like activity, which could catalyze the oxidation of TMB by H$_2$O$_2$ to produce blue color and the catalytic activity was strongly dependent on pH and temperature. Based on papain peroxidase-like catalytic activity and GOx, a simple, cheap, and highly selective colorimetric method for the detection of glucose in human urine samples was developed. There is no denying that the catalytic efficiency of papain is lower than HRP and some nano-enzymes. However, compared with other reported methods, the suggested method does not need expensive reagents and tedious procedures for preparing nanomaterials. It is expected that this work will open

up the possibility of using papain as a substitute for horseradish peroxidase in biochemistry.

Conflicts of interest

There are no conflicts to declare.

Acknowledgements

References

1 C. K. Wang, J. Y. Li, R. Tan, Q. Q. Wang and Z. X. Zhang, *Analyst*, 2019, **144**, 1831–1839.
2 Y. Y. Sheng, H. L. Yang, Y. Wang, L. Han, Y. J. Zhao and A. P. Fan, *Talanta*, 2017, **166**, 268–274.
3 J. M. Lan, W. M. Xu, Q. P. Wan, X. Zhang, J. Lin, J. H. Chen and J. Z. Chen, *Anal. Chim. Acta*, 2014, **825**, 63–68.
4 X. H. Hu, C. Li, C. Feng, X. X. Mao, Y. Xiang and G. X. Li, *Chem. Commun.*, 2017, **53**, 4692–4694.
5 H. Chen, Y. Sun, Y. F. Li, J. Zhao and Y. Cao, *Microchim. Acta*, 2018, **185**, 451.
6 X. X. Mao, Y. F. Li, P. Han, X. H. Wang, S. Q. Yang, F. Zhang, X. Q. Gong and Y. Cao, *Sens. Actuators, B*, 2018, **267**, 336–341.
7 Y. M. Leng, K. Xie, L. Q. Ye, G. Q. Li, Z. W. Lu and J. B. He, *Talanta*, 2015, **139**, 89–95.
8 Y. M. Leng, K. Jiang, W. T. Zhang and Y. H. Wang, *Langmuir*, 2017, **33**, 6398–6403.
9 J. Chen, Q. Chen, J. Y. Chen and H. D. Qiu, *Microchim. Acta*, 2016, **183**, 3191–3199.
10 J. S. Mu, Y. He and Y. Wang, *Talanta*, 2016, **148**, 22–28.
11 Y. Jv, B. X. Li and R. Cao, *Chem. Commun.*, 2010, **46**, 8017–8019.
12 M. N. Karim, S. R. Anderson, S. Singh, R. Ramanathan and V. Bansal, *Biosens. Bioelectron.*, 2018, **110**, 8–15.
13 J. Chen, J. Ge, L. Zhang, Z. H. Li and L. B. Qu, *Sens. Actuators, B*, 2016, **233**, 438–444.
14 L. Rastogi, D. Karunasagar, R. B Sashidhar and A. Giri, *Sens. Actuators, B*, 2017, **240**, 1182–1188.
15 T. G. Choleva, V. A. Gatselou, G. Z. Tsogas and D. L. Giokas, *Microchim. Acta*, 2018, **185**, 22.
16 H. Y. Shin, B. G. Kim, S. Cho, J. Lee, H. B. Na and M. Kim, *Microchim. Acta*, 2017, **184**, 2115–2122.
17 J. S. Mu, Y. Wang, M. Zhao and L. Zhang, *Chem. Commun.*, 2012, **144**, 2540–2542.
18 X. W. Cheng, L. Huang, X. Y. Yang, A. A. Elzatahry, A. Alghamdi and Y. H. Deng, *J. Colloid Interface Sci.*, 2019, **535**, 425–435.
19 L. J. Huang, W. X. Zhu, W. T. Zhang, K. Chen, J. Wang, R. Wang, Q. F. Yang, N. Hu, Y. R. Suo and J. L. Wang, *Microchim. Acta*, 2018, **185**, 7.
20 F. Nekouei, S. Nekouei, O. Jashnsaz and M. Pouzesh, *Mater. Sci. Eng. C*, 2018, **90**, 576–588.
21 C. P. Ding, Y. H. Yan, D. S. Xiang, C. L. Zhang and Y. Z. Xian, *Microchim. Acta*, 2016, **183**, 625–631.
22 Q. Zhong, Y. Chen, A. Su and Y. Wang, *Sens. Actuators, B*, 2018, **273**, 1098–1102.
23 B. Wang, F. Liu, Y. Y. Wu, Y. F. Chen, B. Wen and C. M. Li, *Sens. Actuators, B*, 2018, **255**, 2601–2607.
24 Y. J. Long, X. L. Wang, D. J. Shen and H. Z. Zheng, *Talanta*, 2016, **159**, 122–126.
25 P. K. Yadav, V. K. Singh, S. Chandra, D. Bano, V. Kumar, M. Talat and S. H. Hasan, *ACS Biomater. Sci. Eng.*, 2019, **5**, 623–632.
26 M. L. Lin, Y. J. Guo, Z. Y. Liang, X. S. Zhao, J. N. Chen and Y. L. Wang, *Microchem. J.*, 2019, **147**, 319–323.
27 Y. J. Pang, Z. L. Huang, Y. F. Yang, Y. J. Long and H. Z. Zheng, *Spectrochim. Acta, Part A*, 2018, **189**, 510–515.
28 Y. D. Pan, Y. F. Yang, Y. J. Pang, Y. Shi, Y. J. Long and H. Z. Zheng, *Talanta*, 2018, **185**, 433–438.
29 J. F. Lucas, D. Castaneda and D. Hormigo, *Trends Food Sci. Technol.*, 2017, **68**, 91–101.
30 S. Y. Liu, M. Holdrich, A. S. Engler, J. Horak and M. Lammerhofer, *Anal. Chim. Acta*, 2017, **963**, 33–43.
31 Y. J. Gu, M. L. Zhu, Y. L. Li and C. H. Xiong, *Int. J. Biol. Macromol.*, 2018, **112**, 1175–1182.
32 S. Kim, J. Lee, S. Jang, H. Lee, D. Sung and J. Chang, *Biochem. Eng. J.*, 2016, **105**, 406–411.
33 D. Ji, Y. Du, H. Meng, L. Zhang, Z. Huang, Y. Hu, J. Li, F. Yu and Z. Li, *Sens. Actuators, B*, 2018, **256**, 512–519.
34 J. Ge, K. Xing, X. Geng, Y. L. Hu, X. P. Shen, L. Zhang and Z. H. Li, *Microchim. Acta*, 2018, **185**, 559.
35 R. Grinyte, G. Garai-Ibabe, L. Saa and V. Pavlov, *Anal. Chim. Acta*, 2015, **881**, 131–138.
36 X. Q. Zhang, S. W. Gong, Y. Zhang, T. Yang, C. Y. Wang and N. Gu, *J. Mater. Chem.*, 2010, **20**, 5110–5116.
37 Y. Yang, D. Shen, Y. Long, Z. Xie and H. Zheng, *Sci. Rep.*, 2017, **7**, 43141.
38 B. S. Batule, K. S. Park, S. Gautam, H. J. Cheon, M. Kim and H. G. Park, *Sens. Actuators, B*, 2019, **283**, 749–754.
39 Z. F. Gao, A. Y. Ogbe, E. E. Sann, X. D. Wang and F. Xia, *Talanta*, 2018, **180**, 12–17.
40 X. H. Duan, Q. Liu, G. N. Wang and X. G. Su, *J. Lumin.*, 2019, **207**, 491–496.
41 S. L. Shen, M. M. Jia, Z. H. Tang, S. Chang, P. Y. Shi and J. H. Yang, *Mater. Res. Bull.*, 2018, **144**, 471–477.
42 N. Wang, J. C. Sun, L. J. Chen, H. Fan and S. Y. Ai, *Microchim. Acta*, 2015, **182**, 1733–1738.
43 Q. Q. Wang, X. P. Zhang, L. Huang, Z. Q. Zhang and S. J. Dong, *ACS Appl. Mater. Interfaces*, 2017, **9**, 7465–7471.
44 L. Zhang, X. Hai, C. Xia, X. W. Chen and J. H. Wang, *Sens. Actuators, B*, 2017, **248**, 374–384.
45 L. P. Lin, X. H. Song, Y. Y. Chen, M. C. Rong, T. T. Zhao, Y. R. Wang, Y. Q. Jiang and X. Chen, *Anal. Chim. Acta*, 2015, **869**, 89–95.